Journal of Hydraulic Research Vol. 47 Extra Issue (2009), pp. 126–134
doi:10.3826/jhr.2009.0011

SPH high-performance computing simulations of rigid solids impacting the free-surface of water

Calcul haute performance de l'impact de corps solides sur la surface libre de l'eau par la méthode SPH

PIERRE MARUZEWSKI, *Ecole polytechnique fédérale de Lausanne, EPFL, Laboratoire de machines hydrauliques, LMH, Avenue de cour, 33 bis, 1007 Lausanne, Switzerland. Tel.: +41 216392510; e-mail: pierre.maruzewski@epfl.ch (author for correspondence)*

DAVID LE TOUZÉ, *Ecole Centrale Nantes/CNRS, Fluid Mechanics Laboratory, 1 rue de la Noë, F-44300 Nantes Cedex 3 France. Tel.: +33240371631; e-mail: david.letouze@ec-nantes.fr*

GUILLAUME OGER, *HydrOcean, 1 Rue de la Noë CS 32122 F-44321 Nantes cedex 3 France. Tel.: +3324206084; e-mail: guillaume.oger@hydrocean.fr*

FRANÇOIS AVELLAN, (IAHR Member), *Ecole polytechnique fédérale de Lausanne, EPFL, Laboratoire de machines hydrauliques, LMH, Avenue de cour, 33 bis, 1007 Lausanne, Switzerland. Tel.: +41 216932524; e-mail: francois.avellan@epfl.ch*

ABSTRACT
Numerical simulations of water entries based on a three-dimensional parallelized Smoothed Particle Hydrodynamics (SPH) model developed by Ecole Centrale Nantes are presented. The aim of the paper is to show how such SPH simulations of complex 3D problems involving a free surface can be performed on a super computer like the IBM Blue Gene/L with 8,192 cores of Ecole polytechnique fédérale de Lausanne. The present paper thus presents the different techniques which had to be included into the SPH model to make possible such simulations. Memory handling, in particular, is a quite subtle issue because of constraints due to the use of a variable-h scheme. These improvements made possible the simulation of test cases involving hundreds of million particles computed by using thousands of cores. Speedup and efficiency of these parallel calculations are studied. The model capabilities are illustrated in the paper for two water entry problems, firstly, on a simple test case involving a sphere impacting the free surface at high velocity; and secondly, on a complex 3D geometry involving a ship hull impacting the free surface in forced motion. Sensitivity to spatial resolution is investigated as well in the case of the sphere water entry, and the flow analysis is performed by comparing both experimental and theoretical reference results.

RÉSUMÉ
La simulation numérique de l'impact d'un solide sur une surface libre d'eau faisant appel à la méthode Smoothed Particle Hydrodynamics (SPH) par un modèle 3D parallèle développé par l'Ecole Centrale Nantes est présentée. Le but de 1'article est de montrer comment de telles simulations SPH de problèmes tri-dimensionnels complexes à surface libre peuvent être conduites dans le domaine du Calcul Haute Performance sur un super calculateur tel que 1'IBM Blue Gene/L de l'Ecole polytechnique fédérale de Lausanne, doté de 8,192 cœurs. Cet article présente ainsi les différentes techniques apportées au modèle SPH pour le rendre apte à de telles simulations. La gestion de la mémoire, en particulier, est assez délicate de par l'utilisation de la longueur de lissage variable h. Cette nouvelle gestion de la mémoire a permis la simulation de cas-tests contenant des centaines de millions de particules réparties sur plusieurs milliers de cœurs. L'efficacité et l'accélération de ces simulations parallèles sont étudiées. Les capacités du modèle sont illustrées dans ce papier sur deux exemples d'impact sur la surface libre. Le premier exemple représente le cas simple d'une sphère rigide chutant dans l'eau à grande vitesse. Le second exemple met en avant la possibilité de simuler des géométries plus complexes telles l'impact de la coque d'un bateau sur l'eau en mouvement forcé. Dans le cas de l'impact de la sphère, la sensibilité à la résolution spatiale utilisée a été aussi étudiée, et une analyse de l'écoulement est menée par comparaison à des résultats expérimentaux et théoriques.

Keywords: Free-surface flows, high Performance computing, hydrodynamic impact, parallelization, scalability, smoothed particle hydrodynamics, water entry.

1 Introduction

The Smoothed Particle Hydrodynamic method is well suited for investigating complex free surface problems of fast dynamics such as the water entry of 3D objects of complex geometry. With respect to classical Level-Set or VOF interface tracking methods, the free surface remains always precisely described by the particles in their Lagrangian motion with no need for capturing/tracking this surface, neither for adapting a mesh locally, nor for simulating the air phase.

Revision received January 23, 2009/Open for discussion until June 30, 2010.

Presently, most of the methods available in the free surface SPH related literature are two-dimensional, and thus do not really suffer from high computational cost difficulties. But actual engineering applications are indeed three-dimensional, which dramatically increases the computational cost, and finally limits the use of the SPH method. At least millions of particles and an efficient parallelization are then required.

Therefore, the SPH method being an explicit method, presents the other asset of a rather straightforward parallelization with respect to the classical Finite Difference Method, Finite Volume Method or Finite Element Method used in Computational Fluid Dynamics (CFD). Ecole Centrale Nantes thus decided to develop efficient 3D parallelized software named SPH-Flow. Its implementation was validated on a Cray XD1 cluster with 48 cores (Oger *et al*. 2007). Several other works have been achieved recently on the topic of very large parallel calculations in CFD. For instance, Sbalzarini has developed a highly efficient parallel particle-mesh library which provides a computational tool for mesh-based methods (Sbalzarini *et al.* 2006). Ecole Polytechnique Fédérale de Lausanne has also shown that SPH parallel simulation is available on High Performance Computing machine like an IBM Blue Gene/L with 8,192 cores (Maruzewski and Shepel 2006). Thus, performing a complete SPH 3D simulation with around one hundred million particles is nowadays possible as shown by Maruzewski *et al.* (2008), or by Moulinec *et al.* (2008) with a different code.

The paper is organized in the following way. First, SPH-Flow is briefly described including the procedure to capture the local pressure on solid boundaries. Then the parallelization of this 3D SPH solver is discussed by analyzing a two-dimensional case for the sake of simplicity and clarity. With respect to previous work in the literature, see e.g. Goozee and Jacobs (2003) or Rabczuk and Eibl (2003), the parallel algorithm presented here is of much greater complexity. Actually, when using variable spatial resolution, the parallelization is much less straightforward. Communication and memory issues become critical, and adequate treatments have to be derived to recover a good efficiency. Finally, the capabilities of this 3D parallel SPH method are illustrated in the paper on two water entry problems, firstly, on a simple test case involving a sphere impacting the free surface at high velocity; and secondly, on a complex 3D geometry involving a ship hull impacting the free surface in forced motion. Spatial resolution sensitivity study and detailed flow analysis are also provided.

2 The solver SPH-Flow

2.1 *Methodology*

The solver SPH-Flow (Oger *et al.* 2007), developed by Ecole Centrale Nantes, relies on a renormalization kernel method and the implementation of an exact Riemann solver of Godunov type as described by Vila *et al.* (1999). The latter presents various advantages such as avoiding artificial viscosity required in standard SPH, decreasing numerical dissipation and increasing stability, in a way inspired from compressible finite-volume schemes. Boundary conditions are imposed using ghost particles. Specific developments have been realized to extend this technique from a flat boundary to an arbitrary 3D shape.

Furthermore, SPH-Flow also integrates a spatially variable smoothing length scheme proposed in Oger *et al.* (2007) which relies on both topologies "Gather and Scatter" presented by Hernquist *et al.* (1989) and updated by Bonet *et al.* (1999). SPH-Flow solves the Navier-Stokes equation in Lagrangian form and it is defined by the following equations:

$$\frac{d\rho_i}{dt} = \rho_i \sum_j \frac{m_j}{\rho_j}(\vec{c}_i - \vec{c}_j)\vec{\nabla} W(\vec{x}_i - \vec{x}_j, h_i) \tag{1}$$

$$\frac{d\vec{c}_i}{dt} = \vec{g} - \sum_j \frac{m_j}{\rho_i \rho_j}[P_i \vec{\nabla} W(\vec{x}_i - \vec{x}_j, h_i) - P_j \vec{\nabla} W(\vec{x}_j - \vec{x}_i, h_j)] \tag{2}$$

This scheme is conservative, as shown in (Oger *et al*. 2007). This variable smoothing length technique is well adapted to the test case of water entry of bodies, providing accuracy in the impact area.

2.2 *Local pressure capture procedure*

Numerous flow problems require the knowledge of local pressure value on solid boundaries. However, the correct evaluation of wall pressure values through SPH formalisms still remains quite a challenging task. The procedure retained in the present investigation is based on a specific treatment related to the sampling of near-boundary particles within a distance d from the boundary that is proportional to the smoothing length h (typically $2h$ to $5h$), and within the width of the sensor, in the vicinity of a generic point M of the boundary as shown in Fig. 1. This area S_{sensor} is an image of a pressure distribution experienced by a pressure sensor during an experimental measurement.

The local pressure at M is finally defined as an average of the sampled-particle pressure values. As a consequence, the approximation tends towards the exact pressure at point M as the sensing surface area tends toward zero. With this definition, the number of particles which contribute to the estimation of the boundary pressure at M is sufficient for obtaining a smooth estimate of

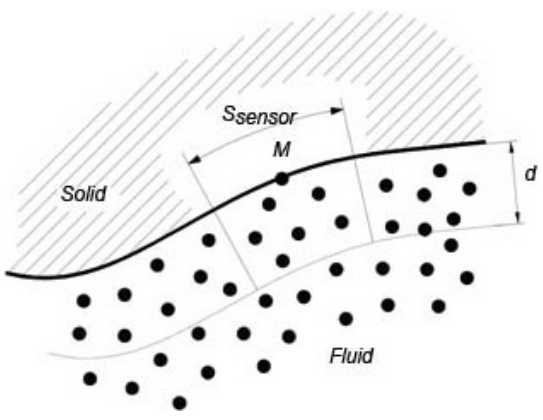

Figure 1 Particle sampling in the vicinity of boundary point M

the mean pressure at this point, determined by Eq. (3) in which an hydrostatic correction is applied depending on the vertical distance between point i' and point M.

$$P_M = \frac{\sum_{i'} P_{i'} dS_{i'}}{\sum_{i'} dS_{i'}} \tag{3}$$

3 High-performance SPH solver

For computational cost saving and memory requirement reasons, the practical implementation of the three dimensional SPH-Flow requires to use its parallel capability. For the sake of simplicity and clarity, the parallelization strategy is discussed in the 2D case two-dimensional point of view; however, the extension to the 3D case is straightforward and is implemented in SPH-Flow.

The domain decomposition consists in splitting the whole fluid domain into sub-domains, each sub-domain corresponding to one dedicated core to which it is allocated at the beginning of the calculation. As its size is adapted during the simulation through a specific algorithm, each process always has approximately the same number of particles to treat, in order to make the global calculation as efficient as possible. Let us consider a given process of interest. This process owns a large number of particles for which it is able to compute the interactions between particles by discrete convolutions everywhere except near the boundaries. Indeed, its neighboring processes contain the missing particles needed for calculating the SPH interpolation sums (1) and (2) close to the process boundary. These missing particles are called "foreign particles". The neighboring processes must therefore communicate to the process of interest the foreign particle data (position, velocity, pressure, etc.) in order to enable it to complete the calculation, namely to account for all of the neighbors of its own particles. Thus, the process of interest has first to communicate to its neighboring processes the limits of the areas, as shown by dotted zones in Fig. 2, including the foreign particles that interact with its own particles. These limits, marked by dashed lines in Fig. 3, are determined from the particles being the closest to the process of interest boundaries, and using the interaction radius,

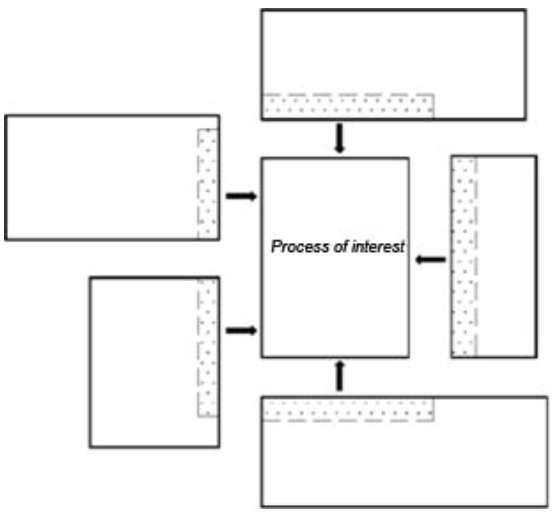

Figure 2 Process of interest with its neighboring processes

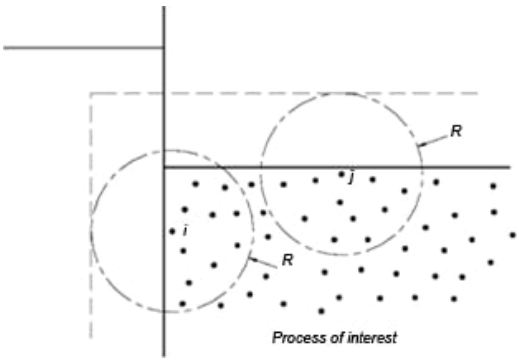

Figure 3 Limits of the foreign particle areas

being equal to twice the largest kernel smoothing length with the chosen cubic spline kernel W. In this process, a dedicated algorithm ensures to get balanced loads afterwards.

The parallelization strategy by domain decomposition is achieved using the standard Message Passing Interface, MPI, library for inter-process communications, with non-blocking communications. The latter is of particular interest since it makes possible to achieve simultaneously any operation, dependent or not on the parallelization itself, and the communications.

Then, the parallel performance of SPH-Flow is evaluated on several fixed-size problems where the smoothing length h is kept constant when increasing the number of cores used, and on a scaled-size problem where h is adapted each time to the number of cores used. In the fixed-size problem, the number of particles is kept constant. Thus, the work load per core decreases with the number of cores. In the scaled-size problem, particle numbers grow proportionally to the number of cores, resulting in a constant load per core.

To evaluate this, parallel performances as timing and parallel efficiency are collected on the Ecole polytechnique fédérale de Lausanne IBM Blue Gene/L, BGL, high performance computer. The 8,192 cores consist of 8 mid-planes packed in 4 racks. Each mid-plane has 512 dual-core computing nodes. Each core is a PowerPC 440 with 512 MB of memory. Then, the elapsed wall-clock time t, the compute speedup S_p and efficiency η for different numbers of particles are measured by Eqs. (4) and (5).

$$S_p(N_{\text{proc}}) = \frac{t(p_{\min})N(N_{\text{proc}})}{t(N_{\text{proc}})N(P_{\min})} \tag{4}$$

$$\eta(N_{\text{proc}}) = \frac{S_p(N_{\text{proc}})}{N_{\text{proc}}} \tag{5}$$

where $P_{\min}$ is the minimal number of cores, linearly extrapolated if not measured, N_{proc} the number of used cores, $N(p_{\min})$ the problem size on $p_{\min}$ cores and $N(N_{\text{proc}})$ the problem size on N_{proc} cores.

4 Impact of a snooker ball

The three dimensional water entry problems are very complex in terms of flow evolution. The present section studies the academic case of a sphere, for instance a snooker ball, impacting the free surface of water, as described experimentally by Laverty (2003),

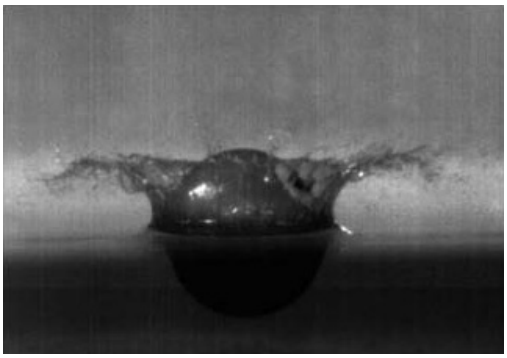

Figure 4 Impact of snooker ball, picture by Laverty (2003)

see Fig. 4. Though geometrically simple, sphere impacts constitute difficult problems due to predominant three dimensional effects. It is one reason why they have been studied almost only experimentally. The present paper is one of few (Ochi and Motter 1969; Neumann 1977; Taranukha and Chizhiumov 2001; Reu and Wang 2004) where a numerical simulation of the slamming problem is shown and validated.

Nonetheless, through the simulation of this sphere water entry problem the first aim of this paper is to evaluate high performance behavior of the SPH-Flow solver.

In the first case', for the fixed-sized problem, 11 cases starting from $h = 0.076$ m for 124,517 particles to $h = 0.00158$ m for 124,105,571 particles are performed. The largest case with about 124 million particles allows a parallel efficiency of 58% on 2,048 cores. The case with 7.5 million particles exhibits a parallel efficiency of 72% on 128 cores. Finally, the case with 3.5 million particles reaches a parallel efficiency of 87% on 64 cores. The speed-up and parallel efficiency on BGL are plotted in Fig. 5 and Fig. 6 for the fixed-size problem.

In the second case, for the scaled-size problem, the starting smoothing length is equal to 0.076 m and decreases in such a way that the number of particles is multiplied by two between two consecutive simulations, under the constraint to keep a constant load around 120,000 particles per core. It represents the maximum load available for the simulations to fit the memory of the BGL computer nodes. The final case is obtained with 124 million particles on 1,024 cores, which was a limit. Actually, huger case simulations appeared unrealistic due to the structure of the source code and the low memory per core of BGL.

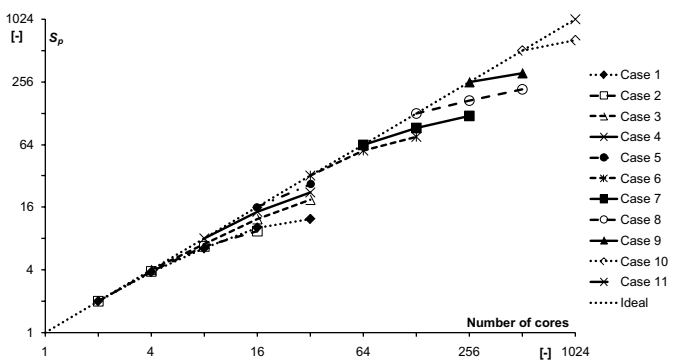

Figure 5 Speedup S_p of fixed-size problems with the 11 cases from 124,517 to 124,105,571 particles

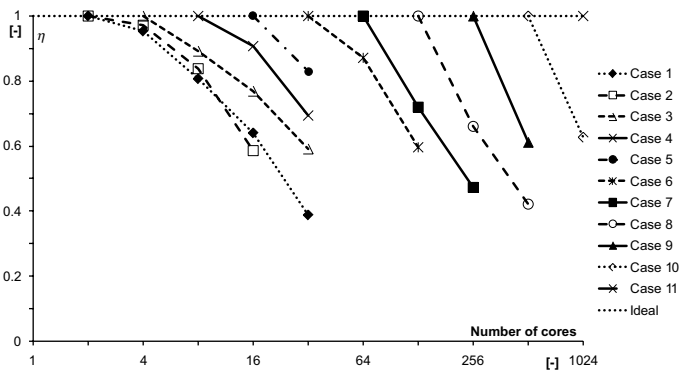

Figure 6 Parallel efficiency η of fixed-size problems with the 11 cases from 124,517 to 124,105,571 particles

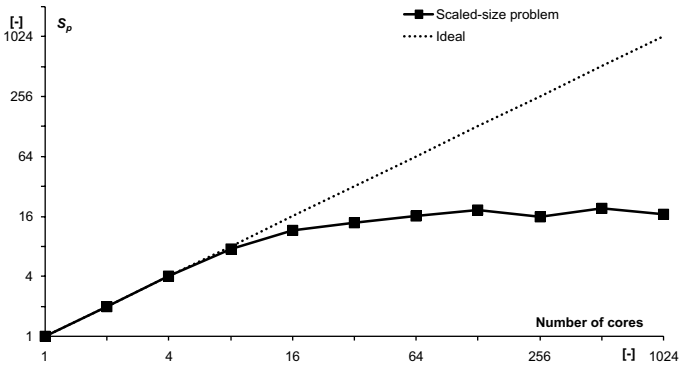

Figure 7 Speed-up Sp of scaled-size problem with a constant load of 120,000 particles per core

The SPH solver SPH-Flow has a very acceptable speed-up until 16 cores for the maximum constant load (almost linear up to 8 cores). For higher number of cores it degrades dramatically. Actually, when performing a simulation with 120,000 particles per core, the computational times obtained are almost unchanged when using from 16 to 1,024 cores, as shown in Fig. 7. By this way, a bottleneck appears between load balancing, cores communications and low memory per core. After investigation, this is mainly due to solid boundary treatment whose parallelization is not fully scalable yet. This has low influence with a few processes, but getting to higher and higher numbers of processes, it becomes a real bottleneck. The implementation of contingency schemes regarding this aspect is presently undergoing and should lead to a much higher scalability.

Thus, the existing parallel implementation proves to be efficient in its principle, showing attractive results (close to linear speedup) for a limited number of cores. This confirms the results which were obtained up to 32 cores on the Cray XD1 cluster of Ecole Centrale Nantes (Oger *et al.* 2007). However, for large numbers of cores, this implementation has to enhanced and/or adapted to the Blue Gene architecture to enable e.g. the simulation of billion particles using all the 8,192 cores of BGL.

4.1 *Sensitivity to spatial resolution*

For investigating, the sensitivity of the calculation to the spatial resolution the SPH computational domain is defined by a rigid

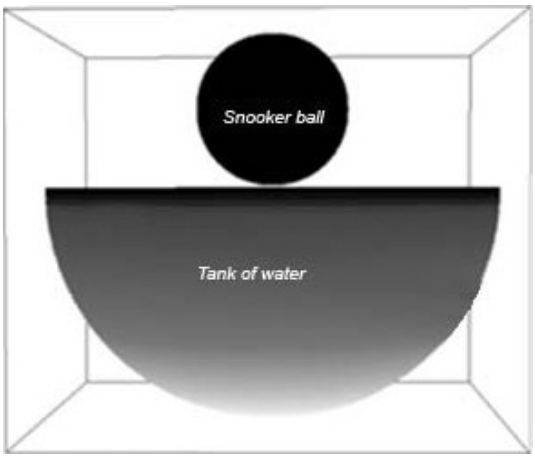

Figure 8 The computational domain

Table 1 Geometric and flow conditions

Water Tank	
Diameter	6 m
Density	1,000 kg · m^{-3}
Snooker Ball	
Diameter	2 m
Impact Velocity	6 m · s^{-1}
Flow Field Properties	
Froude Number *Fr*	1.354

body, the snooker ball, and a half spherical tank of water, as shown in Fig. 8. The physical characteristics of the problem to be solved are summarized in Table 1.

The sensitivity of the predicted flow evolution to the spatial resolution used is estimated by a qualitative evaluation of the capability of the simulations to capture free surface details. The spatial resolution is described in terms of the size of the compact support of the smoothing kernel function W, measured by the smoothing length h which is proportional to the mean particle interspaces. Decreasing the smoothing length h means increasing the number of particles of the computational domain. Three spatial resolutions are used: coarse, medium and fine, with about respectively 80, 200 and 1,200 thousands particles in the corresponding simulations.

The free surface of the water during the impact of the snooker ball is represented for these three spatial resolutions in Fig. 9 to Fig. 11. For coarse resolution, Fig. 9, the impact seems to badly reproduce Laverty's experiment (Laverty 2003) showing insufficient splash-up with respect to Fig. 4, though the impact velocity is the same. In particular, the free surface jets are much less developed. At medium resolution, the characteristic shape of the jets appears, but their amplitude remains under evaluated.

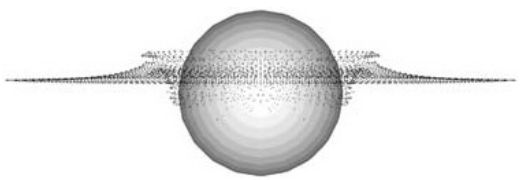

Figure 9 Coarse, $h = 0.09$ m, 82,161 particles

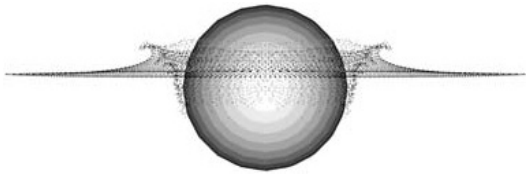

Figure 10 Medium, $h = 0.0625$ m, 197,193 particles

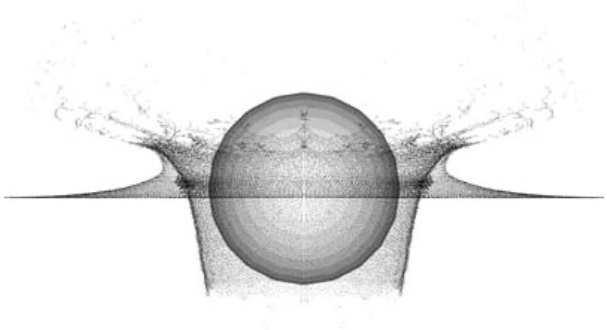

Figure 11 Fine, $h = 0.025$ m, 1,235,279 particles

However, for fine resolution, Fig. 11, the large jets are much more developed, and a crown of thin jets appears on top of the large ones, resulting in the realizing of small drops of water. This result is this time in good agreement with Laverty's experimental result shown in Fig. 4, and with Richardson's measurements (Richardson 1948).

Then, the flow analysis of the sphere impact is performed with the finest spatial resolution used above (1,235,279 particles) for a good description of the flow evolution. In the first hand, the following flow analysis allows understanding the behavior of impact pressures by looking at 4 probes located on the bottom part of the sphere, at 0.1 m, 0.2 m, 0.3 m and 0.4 m from the vertical axis. In the second hand, it is interesting to compare the coefficient which governs the impact force with the literature.

The detail of flow evolution during the snooker ball impact with the fine resolution are shown from Fig. 12 at $t = 0$ s to Fig. 16 at $t = 0.4$ s.

Both the full fluid domain and a vertical section at the center of the domain are shown, enabling to observe both the free surface

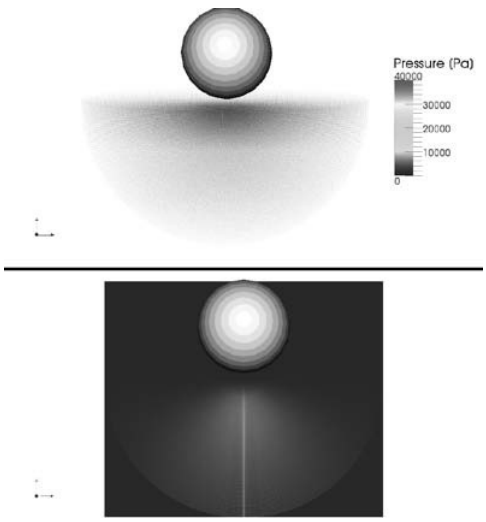

Figure 12 Snooker ball impact at $t = 0$ s

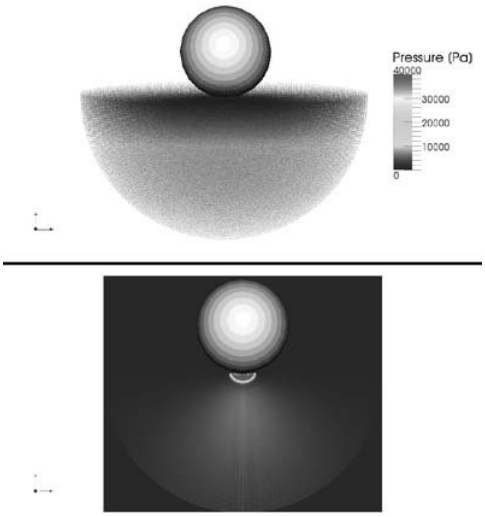

Figure 13 Snooker ball impact at $t = 0.014$ s

and internal pressure field time history evolution. Visualization is performed with the open source ParaView-Meshless software developed at CSCS (Biddiscombe 2007).

At $t = 0$ s, in Fig. 12, the water is in hydrostatic state and the snooker ball starts going vertically downward with a constant velocity of $6\,\mathrm{m}\cdot\mathrm{s}^{-1}$.

At $t = 0.014$ s, in Fig. 13, the snooker ball impinges the free surface of water as shown by the black high pressure spot at the bottom of the ball. The latter reaches the first pressure probe where a high peak is registered at that time, cf. Fig. 17.

The pressure wave then propagates radially downward inside the tank as it can be observed in Fig. 14. Then it reaches the bottom of the water tank at $t = 0.084$.

At $t = 0.132$ s, the pressure wave reaches back the bottom of the sphere, see Fig. 15.

At the end of the simulation, after 0.4 s, the snooker ball reaches the bottom of the tank. The free surface of water is then developed in a large water splash, as described before, see Fig. 16.

To further analyze the flow evolution, it can be looked at the behavior of the dimensionless coefficient which governs the

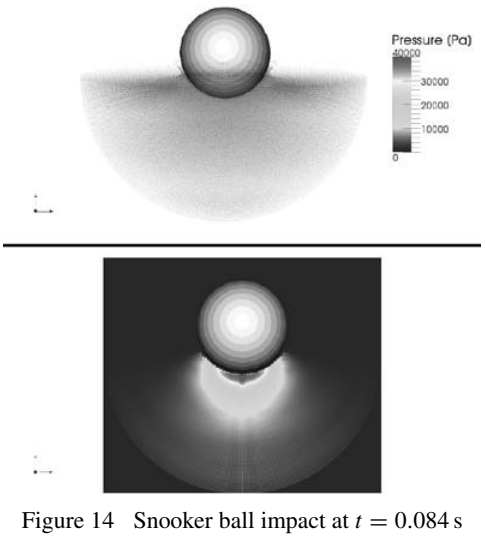

Figure 14 Snooker ball impact at $t = 0.084$ s

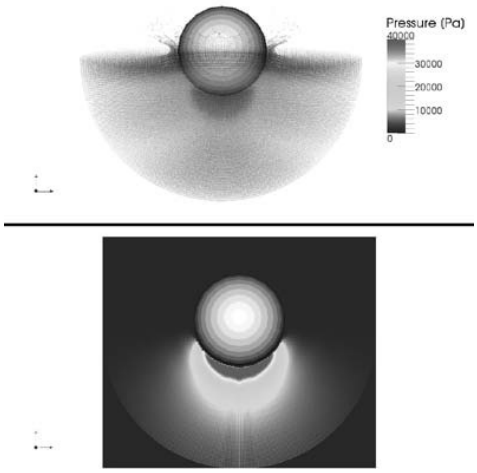

Figure 15 Snooker ball impact at $t = 0.132$ s

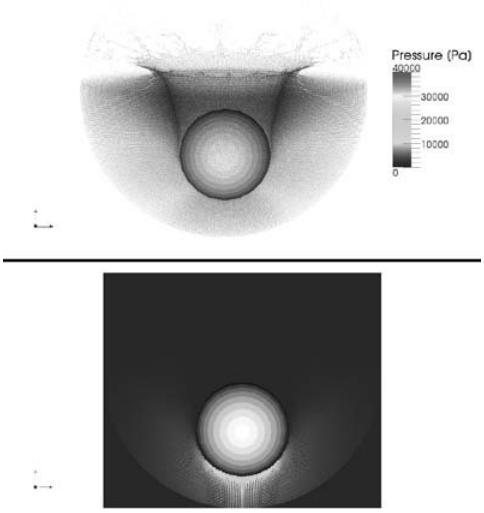

Figure 16 Snooker impact at $t = 0.4$ s

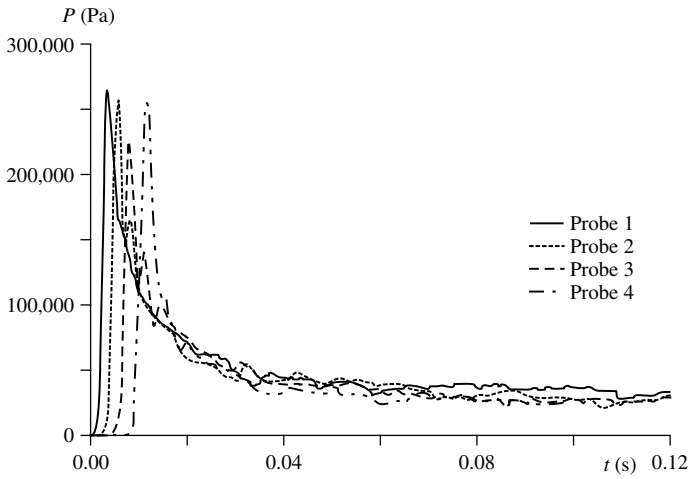

Figure 17 Time dependent local pressure profile along four probes located at the bottom of the snooker ball

impact force: the impact or slamming coefficient, C_s. This coefficient for a sphere impact of constant velocity entry c is defined by Eq. (6).

$$C_s = \frac{F_I}{\frac{1}{2}\rho c^2 \pi R^2} \tag{6}$$

In 1929, Von-Kármán, first, introduced an approximation of C_s by assuming the free surface to be flat and steady throughout the impact process (Von Kármán 1929). The resulting Von-Kármán C_{s-VK} is defined by Eq. (7).

$$C_{s-VK} = 3.30\left(\frac{ct}{R}\right)^{1/2} \tag{7}$$

In 1932, Wagner updated Von-Kármán coefficient by taking into account the deformation of the free surface of the water (Wagner 1932). The resulting Wagner C_{s-W} is defined by Eq. (8).

$$C_{s-W} = 6.03\left(\frac{ct}{R}\right)^{1/2} \tag{8}$$

In 1991, Miloh added a correcting surface wetting factor to the previous formulation (Miloh 1991). He defined the new analytical formulation, called Generalized Wagner formulation, and given in Eq. (9).

$$C_{s-M} = \frac{8\sqrt{2}}{\pi}C_w^{\frac{3}{2}}\left(\frac{ct}{R}\right)^{\frac{1}{2}} - 2.38C_w^2\left(\frac{ct}{R}\right) - 2.0925C_w^{\frac{5}{2}}\left(\frac{ct}{R}\right)^{\frac{3}{2}} \tag{9}$$

where

$$C_w = 1.327 - 0.154\left(\frac{ct}{R}\right) \tag{10}$$

In 2004, Laverty added new terms in the Generalized Wagner impact coefficient by taking into account the buoyancy force, as a function of immersion depth, and the added mass of the sphere, to compare to his experimental results. With this formula, Laverty obtained a very close agreement to his direct experimental measure through Eq. (6).

$$C_s = \frac{mg - \rho g\left[\pi R C_w^2 D^2(t) - \frac{1}{3}\pi C_w^3 D^3(t)\right]}{\frac{1}{2}\rho c^2 \pi R^2} + C_{s-M} \tag{11}$$

Then, the SPH impact coefficient C_{SPH} defined by Eq. (6) is compared to the Von-Kármán, Wagner, and Generalized Wagner laws and Laverty's experimental impact coefficients. The resulting plot of the impact coefficient versus the dimensionless depth is shown in Fig. 18. The SPH simulation is in good agreement with the most complete theories by Miloh and Laverty until a dimensionless depth of 0.3, and so also with the experiments which are very close to Eq. (11) results, (Laverty 2003). The simpler theories by Von-Kármán and Wagner lack of description of the flow evolution after the first stage of the impact. For higher dimensionless depths, SPH results diverge from Miloh and Laverty formulations. This latter difference is explained by the fact that a constant velocity is imposed in the SPH simulation, and the viscous effects are not taken into account, whereas Laverty considered a free fall where the velocity was depending from the elevation.

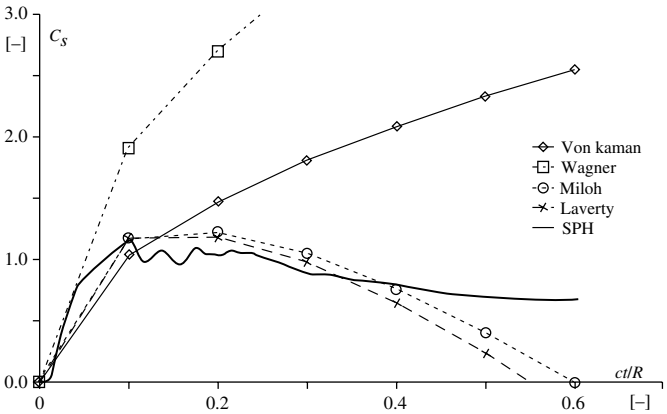

Figure 18 Impact coefficient versus dimensionless depth

5 Impact of a ship Hull

This section presents a validation on the more complex case of a hull shape impacting the free surface of the water in forced motion. The experiments concerning this test case have been performed in the large wave tank, 50 m × 30 m × 5 m of the Fluid Mechanics Laboratory of Ecole Centrale Nantes, ECN. A very good repeatability was obtained during the experiments. To the authors' knowledge, such a comparison with experimental results on this problem has never been shown in the literature even though some simulation attempts have been made, see e.g. the work done by Aquelet *et al.* following their paper (Aquelet *et al.* 2006).

The SPH simulation involves 2,400,000 particles. It has been performed on 16 cores during 24 hours on the Cray XD1 cluster of ECN. Figure 19 presents the calculated free surface evolution during the impact of the ship hull.

This test case represents a good opportunity to test SPH-Flow on a real engineering application, while most of SPH calculations discussed in the literature remain prototypal and are usually

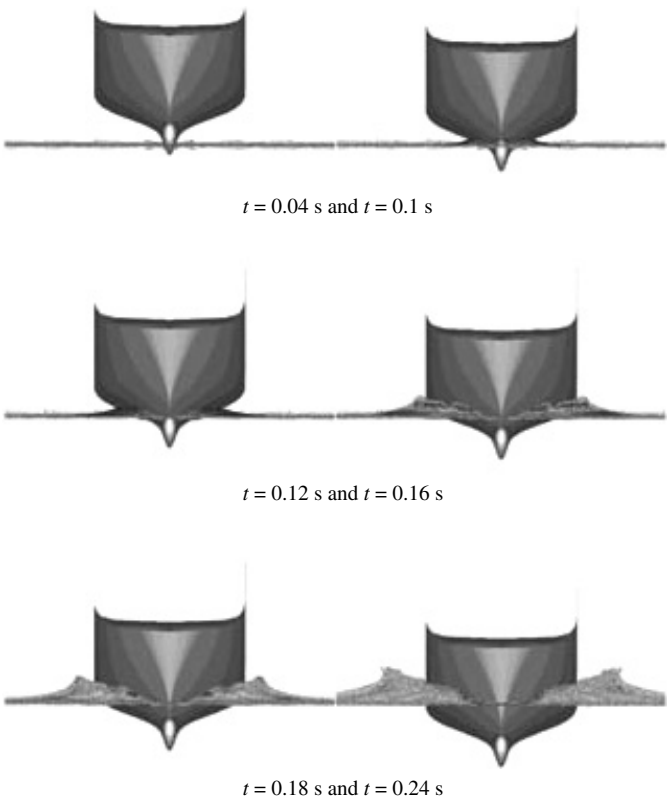

t = 0.04 s and t = 0.1 s

t = 0.12 s and t = 0.16 s

t = 0.18 s and t = 0.24 s

Figure 19 Ship hull impact process

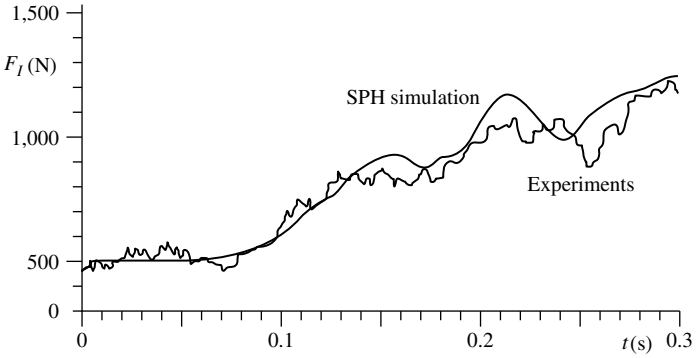

Figure 20 Comparison of impact force between SPH result and ECN experimental database

applied on simple bi-dimensional test cases. The data of interest to be compared with experimental result concerns the time dependent impact force F_I. The SPH predicted force evolution shows a fair agreement with the ECN experimental database, as shown in Fig. 20.

6 Conclusion

In the first hand, this paper presents the implementation and validation of the parallel SPH code, SPH-Flow, on a high performance computer as the Ecole polytechnique fédérale de Lausanne IBM Blue Gene/L. A very good scalability is found up to 16 processes, but the existing SPH code then presents a bottleneck on this architecture when large numbers of cores are used. Nevertheless, a 124 million particles simulation is performed on 1,024 cores. A billion particles simulation is at aim for the near future. In the second hand, the analysis of the impact of rigid bodies on the water free surface at rest is performed. Impact pressure evolution is analyzed through sensors on the sphere and visualization inside the flow. The impact coefficient predicted by SPH simulation of the immersion depth is shown, in good agreement with the analytical formula found in the literature. Finally, a validation on the realistic case of a hull water entry is performed.

Acknowledgement

The authors would like to thank the EPFL High Performance Steering Committee for enabling to perform these numerical simulations on the EPFL Blue Gene Super Computer, the EPFL IT Department, and especially, Christian Clémencon, system manager for his precious advice, and finally John Biddiscombe from CSCS for the development of ParaView-Meshless.

Notation

S = Width of pressure sensor
$\vec{c}$ = Velocity
C_s = Impact coefficient
d = Diameter of sphere or tank
F_I = Impact force
$Fr = \frac{c}{\sqrt{gd}}$ = Froude number
$\vec{g}$ = Gravitational acceleration
h = Kernel smoothing length
m = Particle mass
P = Pressure
R = Radius of sphere
Sp = Speed-up
t = Time
W = Interpolation kernel
$\vec{x}$ = General point
y = Gravitational coordinate
η = Efficiency
ρ = Density

Subscripts
i = Reference particle
i' = Projection of i
j = Neighboring particle

References

Aquelet, N., Souli, M., Olovsson, L. (2006). Euler–Lagrange coupling with damping effects: Application to slamming problems. *Computer Methods in Applied Mechanics and Engineering* 195, 110–132.

Biddiscombe, J. (2007). PV-Meshless Wiki-website.

Bonet, J., Lok, T.S.L. (1999). Variational and momentum preservation aspects of smooth particle hydrodynamics formulations. *Computer Methods in Applied Mechanics Engineering* 180, 97–115.

Goozee, R.J., Jacobs, P.A. (2003). Distributed and shared memory parallelism with a smoothed particle hydrodynamics code. *ANZIAM Journal E* 44, C1–C27.

Hernquist, L., Katz, N. (1989). Treesph: A unification of SPH with the hierarchical tree method. *The Astrophysical Journal Supplement Series* 70, 419–446.

Laverty, S.M. (2003). Experimental hydrodynamics of spherical projectiles impacting on a free surface using high speed imaging techniques, Master in science in ocean engineering at the MIT.

Maruzewski, P., Shepel, S. (2006). The level set interface-tracking model coupled to SPH method. Proc. of the 1st SPHERIC Workshop, Rome, Italy.

Maruzewski, P., Oger, G., Le Touzé, D., Biddiscombe, J. (2008). High performance computing 3D SPH model: Sphere impacting the free–surface of water. Proc. of the IIIrd *SPHERIC* Workshop, 127–133, Lausanne, Switzerland.

Miloh, T. (1991). On the initial-stage slamming of a rigid sphere in a vertical water entry. *Applied Ocean Research* 13, 43–48.

Moulinec, C., Issa, D.R., Marongiu, J.-C., Violeau, D. (2008). Parallel 3-D SPH simulations. *Computing Modeling Engineering Science* 25(3), 133–148.

Neumann, J.N. (1977). Marine Hydrodynamics, MIT Press, 358–373.

Ochi, M.K., Motter, L.E. (1969). Prediction of extreme values of impact pressure associated with ship slamming. *Journal of Ship Research* 13(02), 85–91.

Oger, G., Le Touzé, D., Alessandrini, B., Ferrant, P. (2007). 3D impact flows using an enhanced parallelized SPH model, Proc. Int. Conf. *Violent Flows (VF 2007)*, Fukuoka, Japan.

Oger, G., Doling, M., Alessandrini, B., Ferrant, P. (2007). An improved SPH method: Towards higher-order convergence. *Journal of Computational Physics* 225, 1472–1492.

Rabczuk, T., EibL, J. (2003). Simulation of high velocity concrete fragmentation using SPH/MLSPH. *International Journal for Numerical Methods and Engineering* 56, 1421–1444.

Ren, B., Wang, Y. (2004). Numerical simulation of random wave slamming on structures in the splash zone. *Ocean Engineering* 31, 547–560.

Richardson, E.G. (1948). The impact of a solid on a liquid surface. *Proceedings Physics Society* 61, 352–367.

Sbalzarini, I.F., Walther, J.H., Bergdorf, M., Hieber, S.E., Kotsalis, E.M., Kounoutsakos, P. (2006). PPM A highly efficient parallel particle-mesh library for the simulation of continuum systems. *Journal of Computational Physics* 215, 566–588.

Taranukha, N.A., Chizhiumov, S.D. (2001). Numerical simulation of the fall of a body with a corrugated bottom on water. *Journal of Applied Mechanics and Technical Physics* 42(4), 659–664.

Vila, J.-P. (1999). On particle weighted methods and Smoothed Particles Hydrodynamics. *Mathematical Models and Methods in Applied Sciences* 9, 161–210.

Von Kármán, T. (1929). The impact on seaplane floats during landing, NACA TN 321.

Wagner, H. (1932). Über Stoss und Gleitvorgange an der oberflacke von flüssigkeiten. *ZAMM* (04), 193–235 (In German).